

Chapter 4

Studies on anti-atherosclerosis mechanisms of SR leaf extract

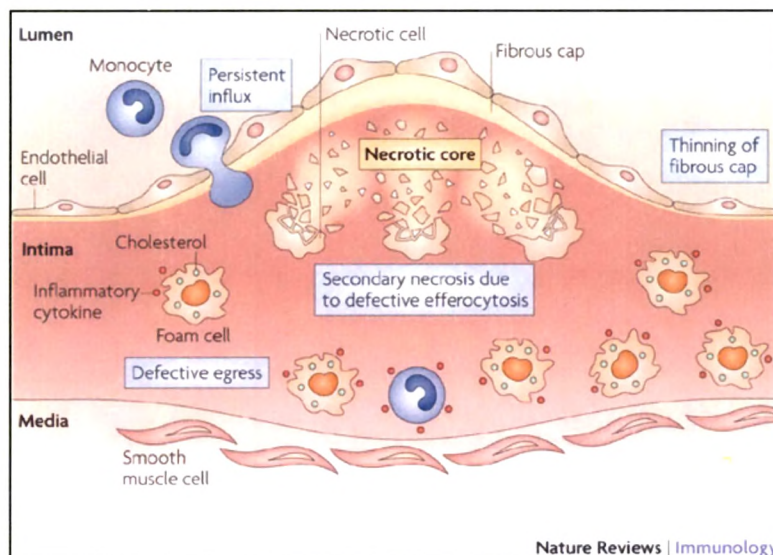
The present study evaluates the development of atherosclerotic lesion in diet induced atherosclerotic rats and the protective role of SR extract on *in vivo* progression of atherosclerosis.

Communicated as: Thounaojam MC, Jadeja RN, Salunke SP, Devkar RV, Ramachandran AV. *Sida rhomboidea*. Roxb leaf extract down-regulates *in vivo* expression of VCAM-1 and P-selectin in atherogenic rats and inhibits *in vitro* macrophage differentiation and foam cell formation. *J Cardiovasc Pharmacol Ther.* (JCPT-2011-Jun-0094)

INTRODUCTION

Atherosclerosis, marked by narrowing of major vessels due to fatty deposition, leads to thrombosis and compromised oxygen supply to target organs (heart and brain). This may eventually precipitate into myocardial infarction or stroke (Libby, 2002). Inflammation is an important component in pathogenesis of atherosclerosis and involves development of an early lesion due to adhesion of leukocytes (particularly monocytes) to the vascular endothelium. Monocytes migrate to the lesion-prone areas of the arterial vasculature and ingest lipids to become foam cells (Jonasson *et al.*, 1986), a hallmark of atherosclerotic plaque formation known as fatty streak.

Figure. 1 Formation of a necrotic core during atherosclerosis.



From: *Nature Reviews Immunology* 10, 36-46 (January 2010) doi:10.1038/nri2675

This leads to lipid laden necrotic core formation caused due to excessive secondary necrosis of macrophages referred to as advanced fibrous lesion (Henson *et al.*,

2000; Tabas *et al.*, 2009). Subsequently, smooth muscle cells start to proliferate and migrate to form a fibrotic cap, consisting of extracellular matrix, collagen, and proteoglycans (Figure.1). A uniformly thick fibrous layer forms a stable plaque but a thin and non-uniform cap may lead to plaque instability. Plaque rupture may result in secondary hemorrhage, thrombosis and occlusion of the artery leading to an important pathophysiological event denoted as complicated lesion (Virmani *et al.*, 2002)

Numerous attempts made over the past 150 years to explain the complex events associated with the development of atherosclerosis has led to the proposition of three distinct hypotheses: 1) the response-to-injury, 2) the response-to-retention, and 3) oxidative modification. Response-to-injury hypothesis of atherosclerosis as proposed by Ross and Glomset (1973) and begins with endothelial injury or dysfunction characterized by enhanced endothelial permeability and LDL deposition in the subendothelial space. This leads to an inflammatory response precipitated by adherence and aggregation of platelets, adhesion and transmigration of leukocytes across the endothelium and foam cell formation. Later, the above set of events form a repetitive vicious cycle resulting in extended lesion and migration of smooth muscle cells into the intima. Finally, development of advanced atherosclerosis occurs characterized by continued macrophage accumulation, fibrous cap formation, and necrosis in the core of the lesion. According to the response-to-retention hypothesis of atherosclerosis, mild to moderate hyperlipidemia causes development of random lesions within the arterial tree characterized by local synthesis of apolipoprotein B-retentive biglycan and decorin. The accumulation of apolipoprotein B-100-containing lipoproteins within the arterial wall is

thought to trigger a proinflammatory cascade. Lipoprotein oxidation may or may not be a part of these responses. Similar to LDL, apolipoprotein B-48-containing chylomicron remnants may also bind to proteoglycans via residues of the apolipoprotein and may be retained within the arterial wall (Proctor *et al.*, 2002). Oxidative modification hypothesis of atherosclerosis opines entrapment of LDL in the subendothelial space and development of lesions followed by oxidative modification by resident vascular cells such as smooth muscle cells, endothelial cells, and macrophages. Oxidized LDL stimulates monocyte chemotaxis, prevents monocyte egress and supports foam cell formation and their necrotic death due to accumulation of oxidized LDL (Diaz *et al.*, 1997).

The present study evaluates the development of atherosclerotic lesion in diet induced atherosclerotic rats and the protective role of SR extract on *in vivo* progression of atherosclerosis.

MATERIALS AND METHODS

Plant material and preparation of extract: as mentioned in chapter 1.

Experimental animals

Male *Sprague Dawley* rats (Obtained from Sun pharmaceutical advanced research centre, Baroda, India), were maintained in clean polypropylene cages and fed with laboratory chow (M/S Pranav agro, Ltd Baroda, India) and provided with water *ad libitum*. The experimental protocol was executed according to the guidelines of the Committee for the Purpose of Control and Supervision of Experiments on Animals (CPCSEA) India and

approved by the animal ethical committee of the Department of Zoology, The M.S. University of Baroda, Vadodara (Approval No.827/ac/04/CPCSEA).

Induction of atherosclerosis

Three groups of eight animals each constituted the experimental set up. Group I served as control (CON) and was fed with standard laboratory chow (Pranav Agro Ltd, Baroda, India) and administered with 0.5 % CMC orally for 8 weeks. Groups II and III were given single dose of Vitamin D3 (600,000 unit/kg, *i.p.*) and later fed with an atherosclerotic (ATH) diet (3% cholesterol, 0.5% cholic acid, 0.2% 6-propyl 2-thiouracil, 5% sucrose, 10% lard, and 81.3% powdered laboratory chow) for 8 weeks (Cai *et al.*, 2005; Wu *et al.*, 2009; Pang *et al.*, 2010). Group III (ATH+SR) also received 200mg/kg SR extract orally while, group II (ATH) received equal volume of vehicle (0.5% CMC).

At the end of the experimental period, rats were fasted overnight and blood collected via retro-orbital sinus puncture in vials. The vials subjected to cold centrifugation (at 4°C at 1500 rpm for 10 min) yielded serum. Later, thoracic aorta, liver, heart and kidney excised from animals sacrificed by cervical dislocation under mild ether anaesthesia were stored at -80°C (Cryo Scientific Ltd, India) for further biochemical analysis.

Serum and aortic lipids: - as mentioned in chapter 1.

Serum autoantibody titre

Serum autoantibody titre was determined as per the method of Uusitupa *et al.* (1996). Ninety six well ELISA plates were coated with 5 µg/mL antigen (Ox-LDL) in PBS (contained 0.27 mmol/L EDTA and 20 µmol/L butylated hydroxytoluene) overnight at

4°C. Plates were then, washed three times with PBS containing 0.5% Tween 20 and twice with water. Non specific sites were blocked with 2% fetal bovine serum (Himedia India, Pvt, Ltd) and washed as above. Serum samples (in PBS containing 1% bovine serum albumin, 0.27 mmol/L EDTA, 20 µmol/L butylated hydroxytoluene, and 0.05% Tween 20) were added on to the plates and were incubated overnight at 4°C followed by washing as mentioned above. Horseradish peroxidase–conjugated human anti-rat IgG (Bangalore Genei, India) at a dilution of 1:200 was added, and plates were incubated at 4°C for 4 hours. After washing, the color developmet was carried out using DAB detection system (Bangalore Genei Pvt Ltd, INDIA) for 10 mins. The reaction was stopped by addition of 2 mol/L H₂SO₄ and, absorbance was read at 492 nm using ELX800 Universal Microplate Reader (Bio-Tek instruments, Inc, Winooski, VT) and expressed as absorbance unit.

Isolation and characterization of LDL

LDL was isolated from serum samples of control and experimental rats by heparin-citrate buffer precipitation method as described earlier by Ahotupa *et al.* (1998). One ml of heparin-citrate buffer (0.064 M tri sodium citrate at pH 5.05 containing 50,000 IU/l heparin) added to 0.1ml serum was mixed on a vortex mixer and allowed to stand for 10 min at room temperature. The insoluble lipoprotein sediment, obtained as a pellet by centrifugation at 3000 rpm for 10 min (at 20°C), was suspended in 1 ml PBS. The method of Lowry *et al.* (1951) using bovine serum albumin as standard helped estimate the protein content of LDL. Assay of MDA and baseline CD (Buege and Aust, 1978; Esterbauer *et al.*, 1989) served the purpose of evaluation of the status of LDL oxidation.

Ex-vivo susceptibility for LDL oxidation and LDL aggregation

Evaluation of *ex-vivo* susceptibility to oxidation involved incubating LDL with Cu²⁺ and continuously monitoring (at 10 min interval for 200min) the formation of conjugated diene at 234nm (Esterbauer *et al.*, 1989).

To determine LDL aggregation, LDL (100 mg protein/L) was vortexed at a fixed strength and absorbance monitored at 680 nm every 10 seconds against a blank (Khoo *et al.*, 1988).

Determination of elastin autofluorescence

For autofluorescence assay, 8µm sections of a frozen piece of thoracic aorta were cut on an IEC Minotome Plus Cryostat, GMI, USA at -20°C. The sections were examined under a Leica DMRB fluorescence microscope using 488 nm filter and photographed using Canon power shot S70 digital camera.

Gross microscopic evaluation of thoracic aorta

Thoracic aorta of control and experimental rats fixed in 4% buffered paraformaldehyde, was dehydrated in graded alcohol series and embedded in paraffin wax using automated tissue processor. Sections of five-µm thickness cut on a microtome were stained with haematoxylin-eosin for microscopic observation. The sections were photographed with a Canon power shot S70 digital Camera at 100 X magnification attached to a Leica microscope.

Calcium localization in thoracic aorta

Paraffin wax sections of control and experimental rats were deparaffinised, hydrated and rinsed in distilled water and incubated in Von Kossa stain solution (1% silver nitrate)

under ultraviolet light for 20 min. The sections were then rinsed repeatedly in distilled water and placed in 5% sodium thiosulphate for 5 min and rinsed in distilled water again (to remove un-reacted silver) before counterstaining with 1% eosin for 5 min (Sheehan and Hrapchak, 1980). Sections examined under a Leica DMRB microscope were then photographed with a Canon power shot S70 digital Camera.

Immunohistochemistry of thoracic aorta

Paraffin embedded sections of thoracic aorta of control and experimental rats were deparaffinised in xylene and hydrated using graded series of alcohol and water. Sections were then washed in PBS and antigen retrieval step was carried out by immersing slides in sodium citrate buffer at 80°C for 10 min. Later, endogenous peroxidase was removed by incubation of sections in 3% H₂O₂ for 20 min in dark. Non-specific binding sites were blocked by incubation of slides with 1% FBS for 30 minutes. Macrophage surface marker (F4/80), VCAM-1, and P-selectin were localized by incubation for overnight at 4°C in a humidified chamber using mouse anti-rat macrophage immunoglobulin (IgG) at a dilution of 1:100 (Santa Cruz Biotechnology, Inc, USA), rabbit anti-rat IgG at a dilution of 1:100 (Santa Cruz Biotechnology, Inc, USA) and, goat anti-rat P-selectin IgG at a dilution of 1:100 (Santa Cruz Biotechnology, Inc, USA) respectively. The sections were incubated with HRP conjugated secondary antibodies for 4 hrs at room temperature. Rabbit anti-mouse IgG-HRP 1:100 (Bangalore Genei Pvt Ltd, INDIA) for macrophage marker, goat anti-rabbit IgG-HRP 1:100 (Bangalore Genei Pvt Ltd, INDIA) for VCAM-1, and rabbit anti-goat IgG-HRP 1:100 (Bangalore Genei Pvt Ltd, INDIA) for P-selectin were used. At the end of incubation, sections were thoroughly washed with PBS and final

detection step was carried out using DAB detection system (Bangalore Genei Pvt Ltd, INDIA) as the chromogen and, sections were counter-stained with haematoxylin. Sections were micro photographed with a canon Power shot S 70 digital camera under Leica DMRB microscope.

Statistical analysis

Statistical evaluation of the data was done by one way ANOVA followed by Bonferroni's multiple comparison test. The results were expressed as mean \pm S.E.M using Graph Pad Prism version 3.0 for Windows, Graph Pad Software, San Diego California USA.

RESULTS

Serum and aortic lipids and autoantibody titre

As shown in Table1, feeding of rats with ATH diet significantly elevated serum levels of TC (73.73%), TG (35.20%), LDL (80.06%), VLDL (34.76%), autoantibody titre (67.96%) and, the levels of aortic TG (56.05%) and TC (74.46%). Concomitantly, serum HDL (37.48%) level was decreased compared to CON rats. However, SR supplementation to ATH diet fed rats significantly minimized these set of changes.

LDL composition, aggregation and ex vivo oxidation

There was a 55.34 % and 71.24 % increment in MDA and CD contents respectively in the LDL samples isolated from ATH diet fed rats (Table.2). Copper mediated oxidation of LDL showed significant resistance in ATH+SR group of rats compared to ATH and CON rats; however, LDL from ATH group showed maximal susceptibility as marked by the significantly lesser lag time compared to CON and ATH+SR rats. Similarly, LDL

sample from ATH rats exhibited maximal aggregation followed by ATH+SR and CON rats in that order (Table.2).

Histopathological observations of thoracic aorta

Photomicrographs of Haematoxylin and eosin (HXE) stained sections of aorta from ATH rats revealed formation of a necrotic core due to accumulation of foam cells, deposition of lipids and loosening of smooth muscle cells in the tunica media (Figure.2, 3 & 4). Von kossa staining revealed calcium deposition in tunica media and intima layers of thoracic aorta of ATH rats. Derangement/defragmentation of elastin layer of tunica media was evident in autofluorescence under green filter (488 nm). However, ATH+SR rats showed no evidence for atheromatous plaque formation and depicted moderate vascular injuries, calcium deposition and elastin derangement (Figure.2, 3 & 4).

Immunohistochemical localization of macrophage marker and cell adhesion molecules

Photomicrographs of sections of thoracic aorta of ATH rats showed intense expression for macrophage marker in atheromatous plaques (Figure. 5, 6 & 7). Cell adhesion molecules (VCAM-1 and p-selectin) also showed elevated levels of expressions in aortic endothelium of ATH rats. However, the expression of macrophage markers and cell adhesion molecules was significantly subdued in thoracic aorta of ATH+SR rats (Figure. 5, 6 & 7).

Table.1 Effect of *S.rhomboidea*.Roxb leaf extract on serum lipid profile and tissue lipids in atherogenic diet fed rats.

	CON	ATH	ATH+SR
Serum			
Cholesterol (mg/dl)	69.67±3.95	265.30±19.12 ^{###}	132.70±13.69 ^{***}
Triglycerides (mg/dl)	61.83±4.23	94.50±7.65 ^{###}	57.33±9.30 ^{***}
High density lipoprotein (mg/dl)	30.60±1.59	19.13±0.91 ^{###}	32.63±2.17 ^{***}
Low density lipoprotein (mg/dl)	51.34±4.02	265.35±12.33 ^{###}	121.53±8.97 ^{***}
Very low density lipoprotein (mg/dl)	12.33±0.99	18.90±1.00 ^{##}	11.45±1.28 ^{**}
Ox-LDL Auto-antibody titre (Optical density)	0.213±0.011	0.665±0.0121 ^{###}	0.337±0.0112 ^{***}
Thoracic aorta			
Cholesterol (mg/g)	5.64±0.45	22.09±1.00 ^{###}	8.04±0.56 ^{***}
Triglycerides (mg/g)	6.21±0.42	14.13±0.71 ^{###}	7.88±0.60 ^{***}

Data expressed as Mean±S.E.M for n=8. Where, ^{##}p<0.01 and ^{###}p<0.001 compared to CON and ^{**}p<0.01 and ^{***}p<0.001 compared to ATH.

Table.2 Effect of *S.rhomboidea*.Roxb leaf extract on LDL oxidation status, lag time during oxidation, LDL aggregation and serum auto-antibody titre against Ox-LDL in atherogenic diet fed rats.

	CON	ATH	ATH+SR
LDL-MDA (nmol/mg LDL protein)	11.23±0.98	25.15±1.23 ^{###}	14.09±1.00 ^{***}
LDL-BCD (nmol/mg LDL protein)	10.09±0.87	35.09±1.41 ^{###}	17.77±1.11 ^{***}
Lag time (min)	14.02±0.99	6.78±0.87 ^{###}	15.66±1.00 ^{***}
LDL Aggregation (%)	100±4.97	230±6.78 ^{###}	110±5.09 ^{***}

Data expressed as Mean±S.E.M for n=8. Where, ^{##}p<0.01 and ^{###}p<0.001 compared to CON and ^{**}p<0.01 and ^{***}p<0.001 compared to ATH.

Figure. 3 Photomicrographs of rat thoracic aorta from control (CON), atherogenic diet fed (ATH) and atherogenic diet fed and treated with *S.rhomboides*.Roxb extract (ATH+SR) stained with haematoxylin and eosin (100X; HXE).

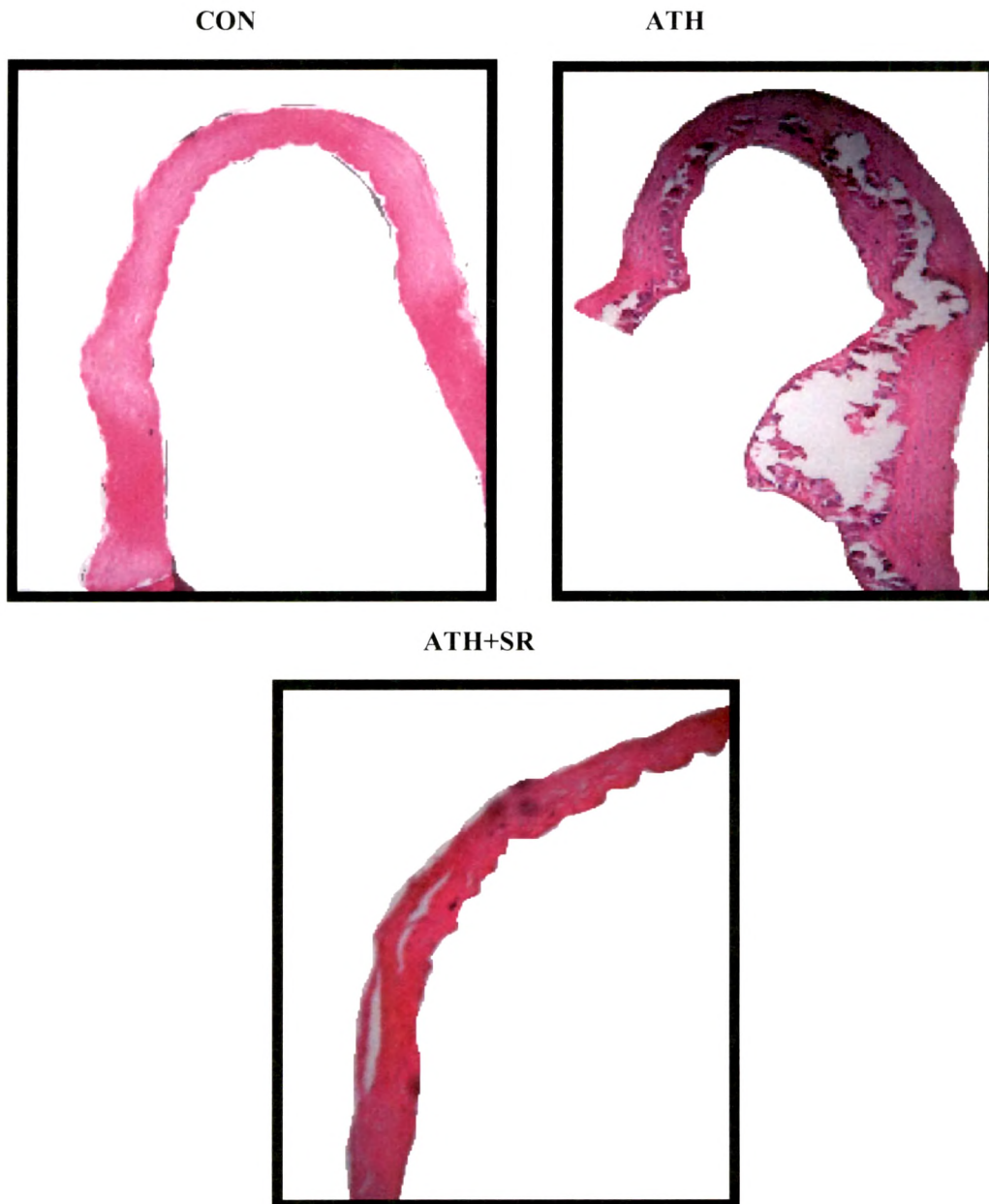
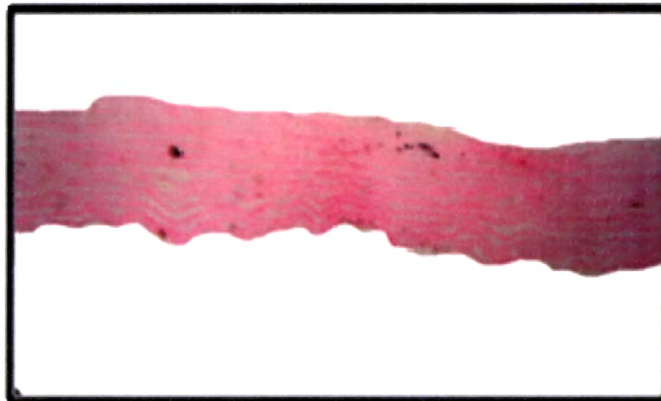


Figure. 4 Photomicrographs of rat thoracic aorta from control (CON), atherogenic diet fed (ATH) and atherogenic diet fed and treated with *S.rhomboidea*.Roxb extract (ATH+SR) depicting elastin auto florescence (200X) and stained with haematoxylin and eosin (100X; HXE) and, von kossa (200X) stains.

CON



ATH



ATH+SR



Figure.5 Photomicrographs of rat thoracic aorta showing immunolocalization of macrophage surface marker (F4/80), VCAM-1 and p-selectin (100X) from control (CON), atherogenic diet fed (ATH) and atherogenic diet fed and treated with *S.rhomboidea*.Roxb extract (ATH+SR).

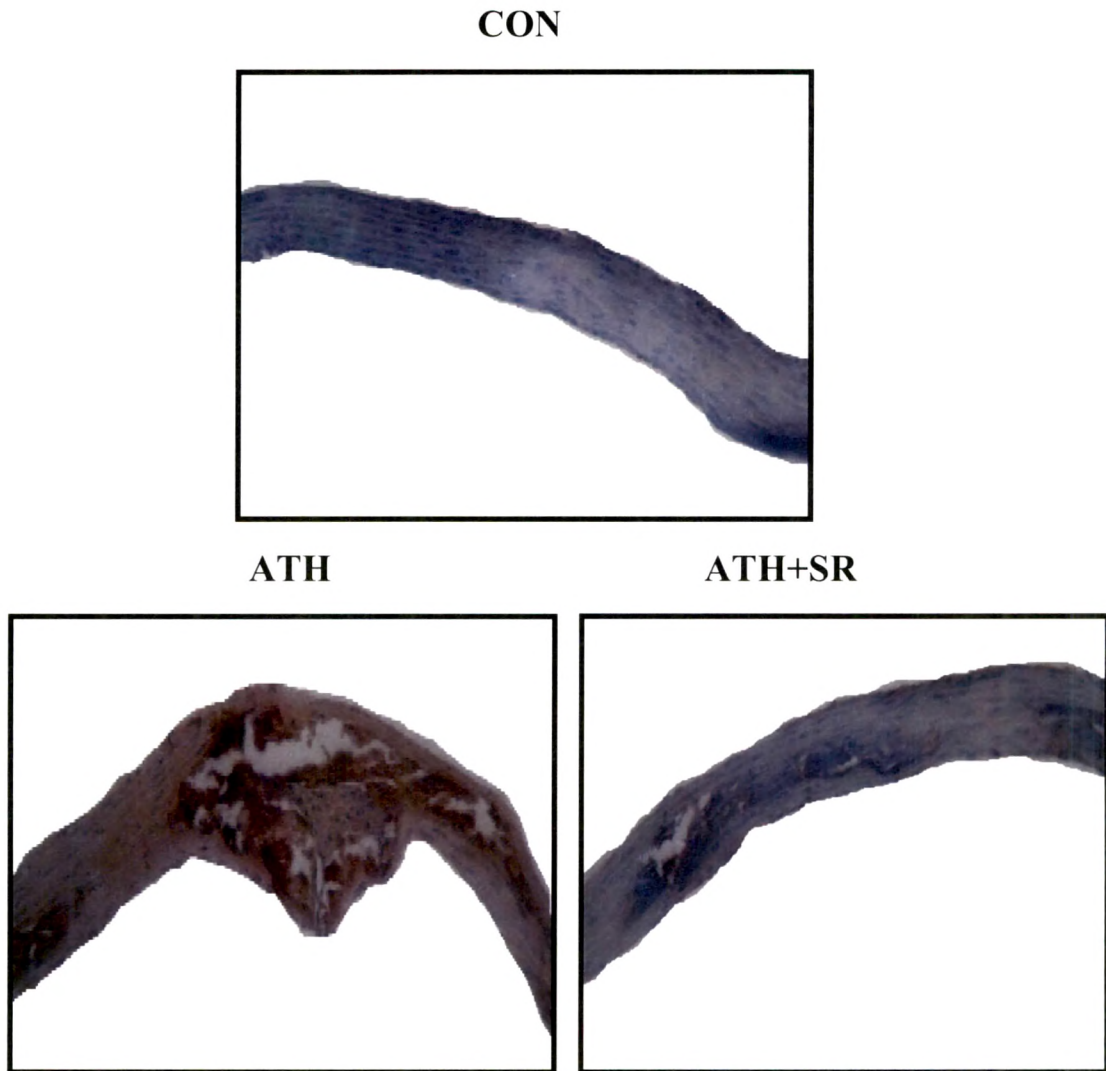


Figure.6 Photomicrographs of rat thoracic aorta showing immunolocalization of vascular cell adhesion molecule-1 (VCAM-1) (400X) from control (CON), atherogenic diet fed (ATH) and atherogenic diet fed and treated with *S.rhomboidea*.Roxb extract (ATH+SR).

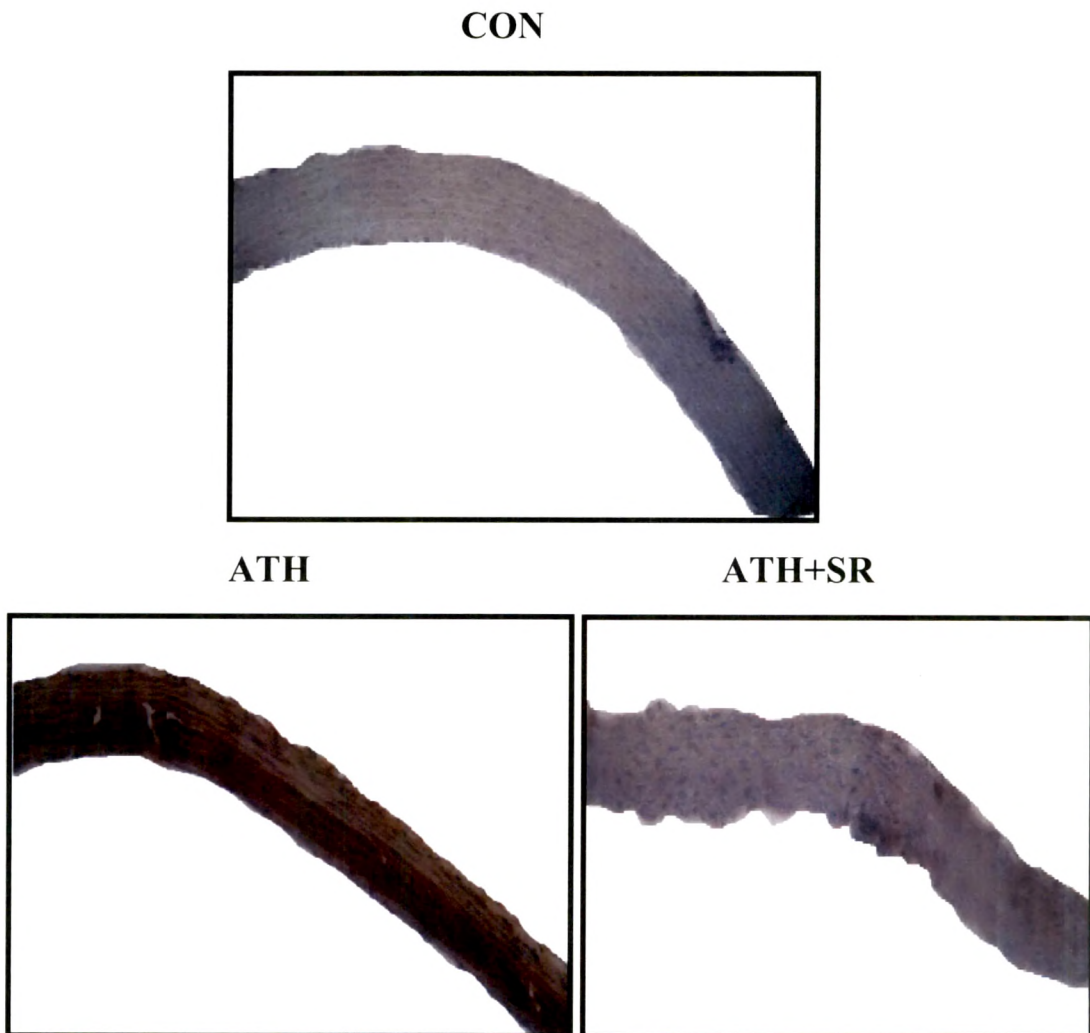
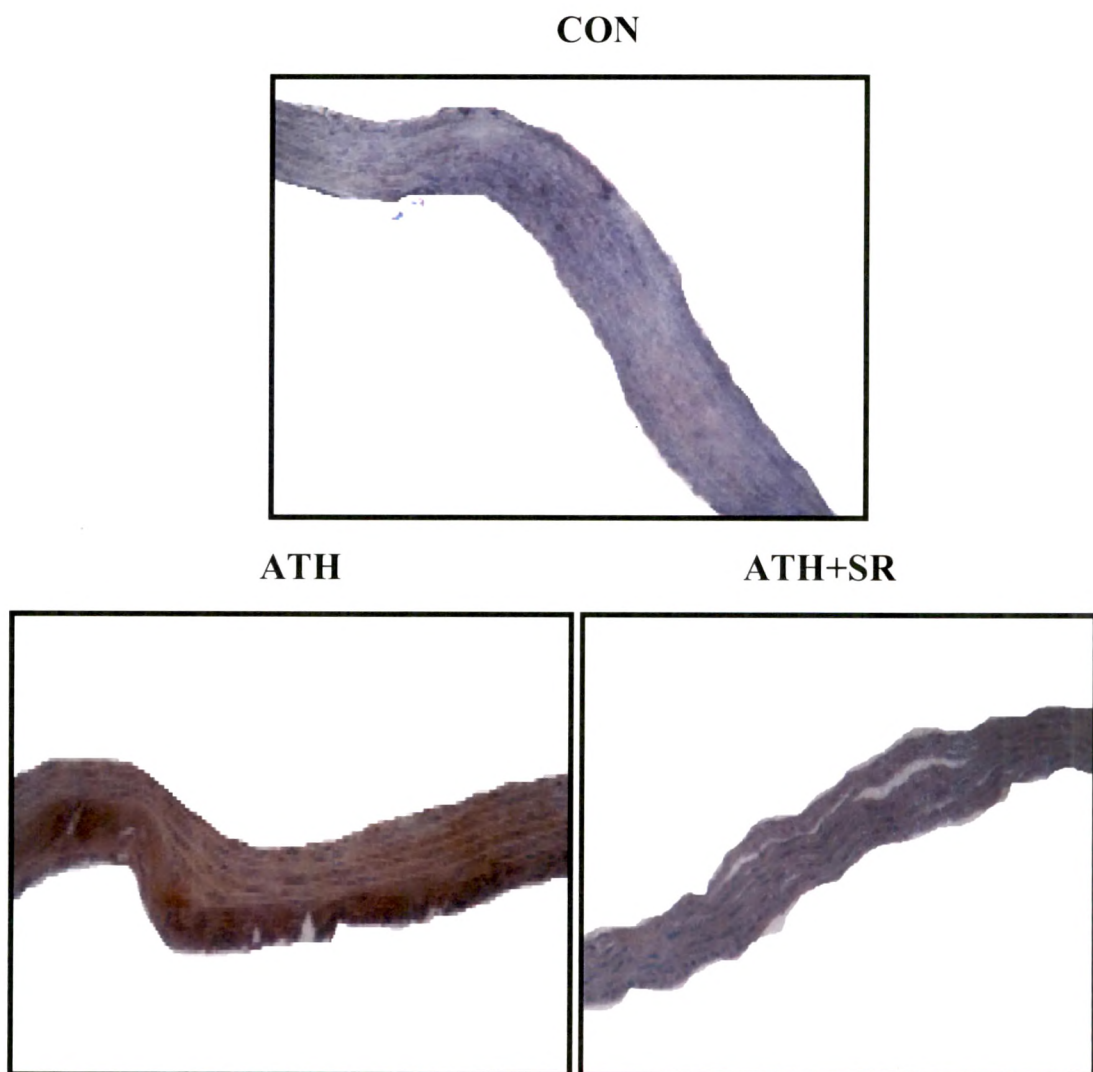


Figure.7 Photomicrographs of rat thoracic aorta showing immunolocalization of p-selectin (100X) from control (CON), atherogenic diet fed (ATH) and atherogenic diet fed and treated with *S.rhomboidea*.Roxb extract (ATH+SR).



DISCUSSION

Hypercholesterolemia plays an important role in the initiation and progression of atherosclerosis and has a positive correlation with cardiovascular disease. Experimental ATH diet fed atherosclerotic model of rats (Cai *et al.*, 2005; Wu *et al.*, 2009; Pang *et al.*, 2010) used in the present study registered significant increment in serum and aortic cholesterol and serum LDL and VLDL along with decrement in HDL. However, co-supplementation with SR extract prevented manifestation of these atherosclerotic changes to a significant extent. These results are in agreement with our previous report on hypocholesterolemic potential of SR extract (Chapter 1). Significant increment of HDL in ATH+SR group is attributable to the previously reported increment in plasma Lecithin-cholesterol acyltransferase activity in SR extract fed hypercholesterolemic rats (Chapter 1). This observation holds great relevance as, low HDL level is a prevalent abnormality in Indian hypercholesterolemic patients (Gupta *et al.*, 1994, 1995) and, synthetic hypocholesterolemic agents have proven to be of negligible significance in elevating HDL level (Wilson, 1990).

Breakdown of polyunsaturated fatty acids and cholesteryl esters forms phospholipids and lipoproteins respectively. These products undergo peroxidation to form highly reactive malondialdehyde (MDA) and 4-hydroxynonenal (4-HNE) (Witztum and Steinberg, 1991) that have ability to form covalent adducts with lysine residues of apoB. Neoepitopes generated by the modification of lysine are immunogenic (Palinski and Witztum, 2000). The titre of antibodies against Ox-LDL (anti-ox LDL antibodies) or MDA-modified LDL is an established marker for predicting propensity of atherosclerosis

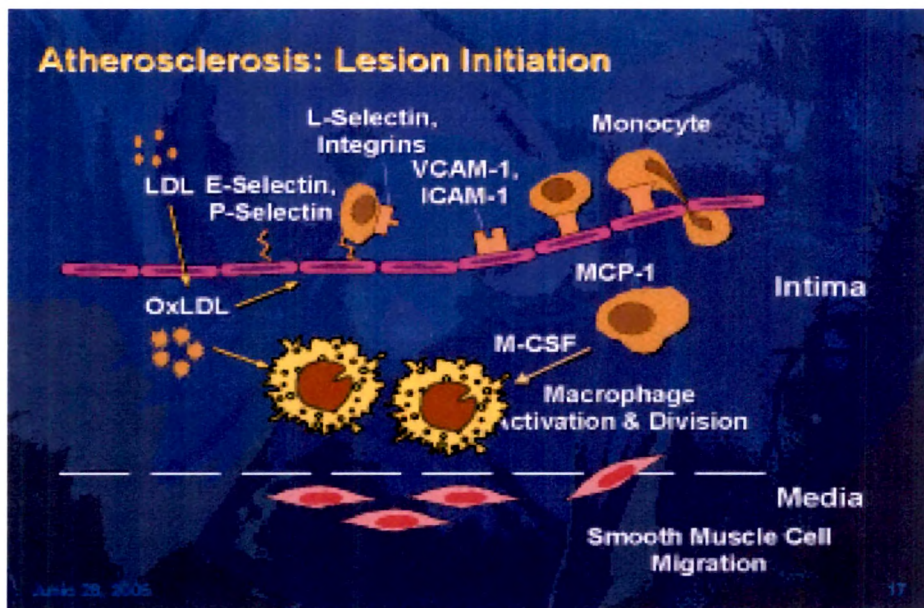
(Geest and Collen, 2001). In a previous study, the ability of SR extract to prevent *in vitro* LDL oxidation was reported (Chapter 5) and hence, presently observed lowering of autoantibody titre against Ox-LDL is in accordance with the same.

Higher indices of MDA and CD in ATH rats confirm *in vivo* LDL oxidation. Further, the relatively shorter lag period recorded for Cu^{2+} mediated *ex vivo* LDL oxidation and higher aggregation tendency provide valuable supportive evidence to the *in vivo* observations. However, supplementation of ATH diet with SR provided significant protection against *in vivo* and *ex vivo* LDL oxidation emphasizing the anti-LDL oxidative potential of SR. These results are in accordance with our previous observation on the antioxidant property of SR extract (Thounaojam *et al.*, 2010b).

Atherosclerotic lesions begin as fatty streaks underlying the endothelium of large arteries. The transition from the relatively simple fatty streak to the more complex lesion appears characterized by the immigration of smooth muscle cells from the medial layer of the artery wall past the internal elastic lamina and into the intimal or sub-endothelial space. Intimal smooth muscle cells may proliferate and take up modified lipoproteins, contributing to foam cell formation and synthesis of extracellular matrix proteins that lead to the development of fibrous cap (Ross, 1999; Steinberg and Witztum, 1999; Paulsson *et al.*, 2000). Clearly, SR extract could effectively prevent the same as validated by the herein recorded minimal macrophage positive areas in the aorta of ATH+SR rats revealed by immunostaining for macrophage marker. This receives adequate confirmation from the *in vitro* observations on monocyte to macrophage differentiation

and the consequent Ox-LDL induced foam cell formation. These observations together highlight the potent anti-atherogenic property of SR extract.

Figure. 8 Role of cell adhesion molecules in atherosclerosis



From: - Kinlay et al. *J Cardiovasc Pharmacol.* 1998;32(suppl 3):S62-S66

Increased expression of adhesion molecules by the activated endothelium is a critical feature of atherosclerosis. It has been reported that feeding of experimental animals with ATH diet rapidly induces VCAM-1 expression in aortic endothelium *in vivo* (Li *et al.*, 1993) and facilitates Ox-LDL induced up-regulation of VCAM-1 in cultured endothelial cells (Khan *et al.*, 1995). VCAM-1 is an immunoglobulin-like adhesion molecule expressed on activated endothelial cells and is capable of binding to $\alpha_4\beta_1$ integrin, constitutively expressed on lymphocytes, monocytes, and eosinophils (Ley and Huo, 2001). Although, it is structurally similar to ICAM-1 and other endothelial adhesion

molecules, the pattern of VCAM-1 regulation is unique. VCAM-1 though not expressed under baseline conditions is rapidly induced by pro atherosclerotic conditions in experimental animals and humans (O'Brien *et al.*, 1993; Nakashima *et al.*, 1998). Another cell adhesion molecule, P-selectin, is a member of the selectin family localized in the membranes of the α -granules of platelets and the Weibel-Palade bodies of endothelial cells (Woollard, 2005). Expressed on the cell surface upon activation, it serves as the first point of contact for adhering of leukocytes to activate platelets present in thrombi or to activate endothelial cells (Figure.8; Woollard and Chin-Dusting, 2007). Considering the importance of cell adhesion molecules, they are the favourite target in recent times for the development of anti-atherogenic drugs/therapy (Haverslag *et al.*, 2008). Consistent with another report (Cai *et al.*, 2005), the present study also validates the expression of cell adhesion molecules (CAMs) on the endothelial surface of atherosclerotic rats, not characteristic of non-atherosclerotic rats. Interestingly, rats fed with SR supplemented ATH diet recorded minimal expression of these CAMs on their aortic endothelium. The results are correlatable with their already reported anti-inflammatory potential (Venkatesh *et al.*, 1999) and, apparently, in addition to its antioxidant property, SR also contributes to overall prevention of atherosclerosis.

Vascular calcification is a common feature of atherosclerotic lesions, considered as an end-stage process of ‘passive’ mineral precipitation. It causes decreased aortic compliance and elastic recoil. In addition, impaired reverse aortic flow and coronary perfusion also, characterize severe cases of cardiac ischemia, (Wallin *et al.*, 2001). Pathological examinations reveal co-localization of vascular calcification within the

atherosclerotic lesions, a stage also referred to as atherosclerotic calcification. Pathological evaluation of thoracic aorta from ATH animals suggest presence of foam cells within the necrotic core as evidenced by HXE staining as well as aortic calcification as evidenced by Von Kossa staining. Concurrently, ATH aorta also depicted disorganization and fragmentation of elastin laminae as evidenced in auto florescence. In contrast, the aorta of ATH+SR rats showed minor calcification and intact elastin lamina but with mild vascular injury that did not develop into a mature plaque. Previous studies had reported augmented *in vitro* and *in vivo* Ox-LDL induced vascular calcification during atherosclerosis (Tang *et al.*, 2006, 2007). In this regard, our previous reports on SR extract induced prevention of LDL oxidation (Chapter 5) and histopathological findings reported in this study stand well correlated and corroborated.

In conclusion, present study demonstrates the potent potential of SR extract in preventing formation and progression of atherosclerotic lesions and provides compelling evidence for its anti-atherogenic property *per se*.

Summary

In the present study effect of *Sida rhomboidea*. Roxb (SR) leaf extract on *in vivo* progression of atherosclerosis was evaluated. Serum and aortic lipid profiles, serum markers of low density lipoprotein (LDL) oxidation and *ex vivo* oxidation of isolated LDL were evaluated in various experimental groups. Also, histopathology and immunolocalization of macrophage marker (F4/80), vascular cell adhesion molecules-1 (VCAM-1) and P-selectin were performed in thoracic aorta of control and treated rats. SR extract treatment to ATH diet fed rats significantly prevented serum and aortic dyslipidemia and increment in serum markers of LDL oxidation and auto-antibody titre. LDL samples isolated from ATH+SR rats showed maximum resistance towards *ex vivo* oxidation and aggregation. Also, microscopic evaluations of thoracic aorta of ATH+SR rats depicted minimal evidence of atheromatous plaque formation, calcium deposition, distortion/defragmentation of elastin and accumulation of macrophages. Expressions of cell adhesion molecules (VCAM-1 and P-selectin) were also down-regulated in ATH+SR rats compared to ATH rats. It can be concluded from the present study that, SR extract is capable of controlling induction of experimental atherosclerosis and warrants further evaluation at clinical level.

Schematic summary

